SUN, SOLAR ACTIVITY, SOLAR-TERRESTRIAL RELATIONS AND ASTROBIOLOGY

https://doi.org/10.18524/1810-4215.2025.38.340497

MORPHOLOGICAL FEATURES OF EXTREME GEOMAGNETIC STORM SOURCES

N. N. Kondrashova, M. N. Pasechnik

Main Astronomical Observatory, NASU, Kyiv, Ukraine,
kondr@mao.kiev.ua, rita@mao.kiev.ua

ABSTRACT. The modern world is becoming increasingly vulnerable to geomagnetic storms due to the rapid development of new technologies and technical systems. This applies to all areas of human activity where power grids, GPS, the Internet, and digital communications are used.

Storms can cause damage to the energy sector, aviation, navigation, satellite electronics, communication systems, industry, and the agro-industrial complex. Extreme geomagnetic storms can cause enormous economic damage and endanger to human health. Their prediction is very important, but not yet perfect enough.

Extreme geomagnetic storms are typically caused by coronal mass ejections (CMEs) during powerful flares. A detailed study of their sources is very important. To study the conditions that favor the occurrence of extreme storms, we selected six active regions (ARs) that were their sources in the period from 2000 to 2024. We have analyzed the spatial and temporal evolution, morphological characteristics, magnetic field structure, and flare activity of NOAA 09393, 10484, 10486, 10501, 10696, 13664. Some ARs were located in large activity complexes.

The ARs studied developed rapidly, their area and number of spots increased, their magnetic structure became more complex, and the flare activity increased. Many of these ARs had very large maximum areas exceeding 2000 millionths of a solar hemisphere. On the days when the eruptions occurred the ARs were located near the central meridian, and the Bz-component of the interplanetary magnetic field was directed south. Their area and spot number were close to their maximum, the magnetic configuration was βγδ in most cases. The sources of the CMEs were M and X class flares, which were preceded by the rapid emergence of new magnetic fluxes and their reconnection with the existing magnetic field of the region.

The most powerful geomagnetic storms during the considered period with a minimum DST index less than -400 nT were observed on November 20, 2003 and May 10–11, 2024. These storms were caused by CMEs from flares occurred in ARs 10501 and 13664. These ARs were characterized by complex magnetic topology and rapid magnetic flux emergence. The storm on May 10–11, 2024, was preceded by cannibal CMEs that enhanced its strength and duration. The most powerful storm of the period under review, on November 20, 2003, with a peak Dst index of -422 nT, was caused by a CME from an M3.9 flare in the AR NOAA 10501. During the storm's peak, auroras were observed as far south as Florida, Michigan, and Wisconsin in the United States and Greece in Europe. It was found that AR with a small area and moderate flares can produce extreme storms, while ARs with large areas and with powerful flares do not always.

Keywords: Sun, active regions, sunspots, solar flares, coronal mass ejections, geomagnetic storms.

АНОТАЦІЯ. Сучасний світ стає дедалі вразливішим до геомагнітних бур через швидкий розвиток нових технологій та технічних систем. Це стосується всіх сфер людської діяльності, де використовуються енергетичні мережі, GPS, Інтернет та цифровий зв'язок. Бурі можуть завдати шкоди енергетиці, авіації, навігації, супутниковій електроніці, системам зв'язку, промисловості та агропромисловому комплексу. Екстремальні геомагнітні бурі можуть завдати величезної економічної шкоди та загрожувати здоров'ю людини. Їх прогнозування дуже важливе, але ще недостатньо досконале.

Екстремальні геомагнітні бурі зазвичай спричинені викидами корональної маси (КВМ) під час потужних спалахів. Детальне дослідження їх джерел є дуже важливим. Для вивчення умов, що сприяють виникненню екстремальних штормів, ми вибрали шість активних областей (АО), які були їх джерелами у період з 2000 по 2024 рік. Ми проаналізували просторову та часову еволюцію, морфологічні характеристики, структуру магнітного поля та спалахову активність АО NOAA 09393, 10484, 10486, 10501, 10696, 13664. Деякі АО знаходилися у великих комплексах активності.

Досліджувані АО розвивалися швидко, їхня площа та кількість плям збільшувалися, магнітна структура ставала складнішою, а спалахова активність зростала. Багато з цих АО мали дуже велику максимальну площу, що перевищувала 2000 мільйонних часток сонячної півкулі. У дні виверження АО розташовувалися поблизу центрального меридіана, а Bz-компонент міжпланетного магнітного поля був спрямований на південь. Їхня площа та кількість плям були близькими до максимуму, магнітна конфігурація в більшості випадків була βγδ. Джерелами КВМ були спалахи класу M та X, яким передував швидкий вихід нових магнітних потоків та їх перез'єднання з уже існуючим магнітним полем області.

Найпотужніші геомагнітні бурі за розглянутий період з індексом геомагнітної активності Dst менше -400 нТл спостерігалися 20 листопада 2003 року та 10–11 травня

2024 року. Бурі були спричинені корональними викидами маси від спалахів, що сталися в АО NOAA 10501 та 13664. Ці АО характеризувалися складною магнітною топологією та швидким виходом магнітного потоку. Бурі 10–11 травня 2024 року передували КВМ типу «канібалізм», які посилили її силу та тривалість. Найпотужніший шторм розглянутого періоду, 20 листопада 2003 року, з піковим індексом Dst = -422 нТл, був спричинений КВМ від спалаху M3.9 в АО NOAA 10501. Під час піку шторму полярні сяйва спостерігалися аж до Флориди, Мічигану та Вісконсина у Сполучених Штатах та Греції в Європі. Було виявлено, що АО з невеликою площею та помірними спалахами можуть спричиняти екстремальні шторми, тоді як АО з великою площею та потужними спалахами не завжди їх викликають.

Ключові слова: Сонце, активні області, сонячні плями, сонячні спалахи, викиди корональної маси, геомагнітні бурі.

1. Introduction

Extreme geomagnetic storms can cause enormous economic damage and threaten human health. The modern world is becoming increasingly vulnerable to geomagnetic storms due to the rapid development of new technologies and technical systems. The first extreme space weather event was observed in early September 1859 by Carrington (Carrington, 1859) and Hodgson (Hodgson, 1859). A very powerful flare on September 1, 1859, caused a severe geomagnetic storm that disrupted telegraph communications in Europe and North America. Auroras were observed all over the world. The Dst (Disturbance Storm Time Index) peak, which provides information about the strength of the ring current around the Earth, was estimated to have ranged from -900 nT to -1640 nT. The X-ray class of the flare that caused the storm is estimated to be X64.4 or ≈X80. Other extreme events were the event of May 13, 1921 (peak Dst=-907 nT), the Fatima geomagnetic storm of January 25-26, 1938. Since 1957, the beginning of the space era, extreme storms with a peak Dst index below -400 nT, were the events of September 13, 1957 (peak Dst = -427 nT), February 11, 1958 (peak Dst = -426 nT), July 15, 1959 (peak Dst = -429 nT). The most powerful geomagnetic storm since that time was the Quebec March 13-14, 1989 (peak Dst = -589 nT).

Forecasting extreme geomagnetic storms is very important, but not yet perfect. To study the conditions that contribute to the occurrence of extreme storms, we selected six active regions that were their sources between 2000 and 2024. We analyzed the spatial and temporal evolution, morphological characteristics, magnetic field structure, and flare activity of NOAA ARs 09393, 10484, 10486, 10501, 10696, 13664. These ARs were the sources of geomagnetic storms with a minimum Dst index near -400 nT.

Magnetograms, continuum images of these ARs were provided by the Solar and Heliospheric Observatory (SOHO) Michelson Doppler Imager (MDI) and the Solar Dynamics Observatory (SDO) Helioseismic and Magnetic Imager (HMI). X-ray data were acquired on the Geostationary Operational Environmental Satellite (GOES). Data on the solar flares are taken from the site https://www.lmsal.com/solarsoft/latest_events_archive.html and data on SMEs and their impact on Earth from the site https://www.swpc.noaa.gov. NOAA's Space Weather Prediction Center (SWPC) is a division of the National Weather Service. Dst indexes of geomagnetic activity are taken from the site of Kyoto geophysical observatory https://wdc.kugi.kyoto-u.ac.jp/dst_final/index.html.

2. Extreme geomagnetic storms of November 20, 2003 and May 10-11, 2024

The most powerful geomagnetic storms since 2000 were the storms on November 20, 2003 and May 10-11, 2024. The geomagnetic storm of May 10-11, 2024, with a peak Dst index of -412 nT, was the most powerful storm since the 2003. This storm was produced by a Carrington-type active region NOAA 13664. The topology of the magnetic field of the active region based on data from the SDO observatory was studied in (Jarolim et al., 2024, Jaswal et al., 2024, Mac Taggart et al., 2024, Romano et al., 2024). The evolution of coronal mass ejections (CMEs) and their geoeffectiveness are reviewed in (Hayakawa et al., 2024, Liu et al., 2024, Wang et al., 2024).

Super active region NOAA 13664 appeared in the southern hemisphere of the solar disk on May 1, 2024, during the phase of increasing solar activity near the maximum of the 25th solar activity cycle. AR 13664 developed very quickly until May 8, 2024. The number of sunspots and the area of AR increased rapidly. From May 4th to 8th, the area of the AR increased from 240 to 630 millionths of the solar hemisphere (designation in the figures – m. s. h.), and the number of sunspots increased from 16 to 37 (Fig. 1b). The maximum area of 2400 millionths of the solar hemisphere was observed on May 11, and the maximum number of sunspots was 81 on May 10.

HMI magnetograms AR 13664, obtained by the SDO on May 6, 7 and 8, 2024, show that the structure of the AR magnetic field changed during this period and became very complicated, of βγδ class (Fig. 1a). On May 6, a new bipole emerged on the AR eastern side, and to the east of it, a small bipolar AR NOAA 13668 appeared nearby. An active complex was formed from these two regions. Fig. 1a also shows the emergence of a bipole with different polarities in the southern and central parts of the AR. Magnetic reconnections began, which caused the powerful flares. On May 8 a series of M- and X-class flares occurred in the AR (Fig. 1c), causing coronal mass ejections, which resulted the extreme geomagnetic storm began on May 10. MacTaggart et al. (2024) showed that an emerging bipole of twisted magnetic field was the source of the X1 flare and the first halo CME. As the authors established, it was a twisted magnetic tube, which subsequently erupted. The event was classified as a G5 geomagnetic storm. The storm became sixth extreme since the beginning of the space age. Proton storm with intensity S2 began on May 10 too. Some CMEs catching up and merged with previous ones to form a cannibal CME, which intensified and prolonged the storm (Liu et al., 2024; Wang et al., 2024). Other cases of cannibal CMEs formation have been studied, for example, in (Soni

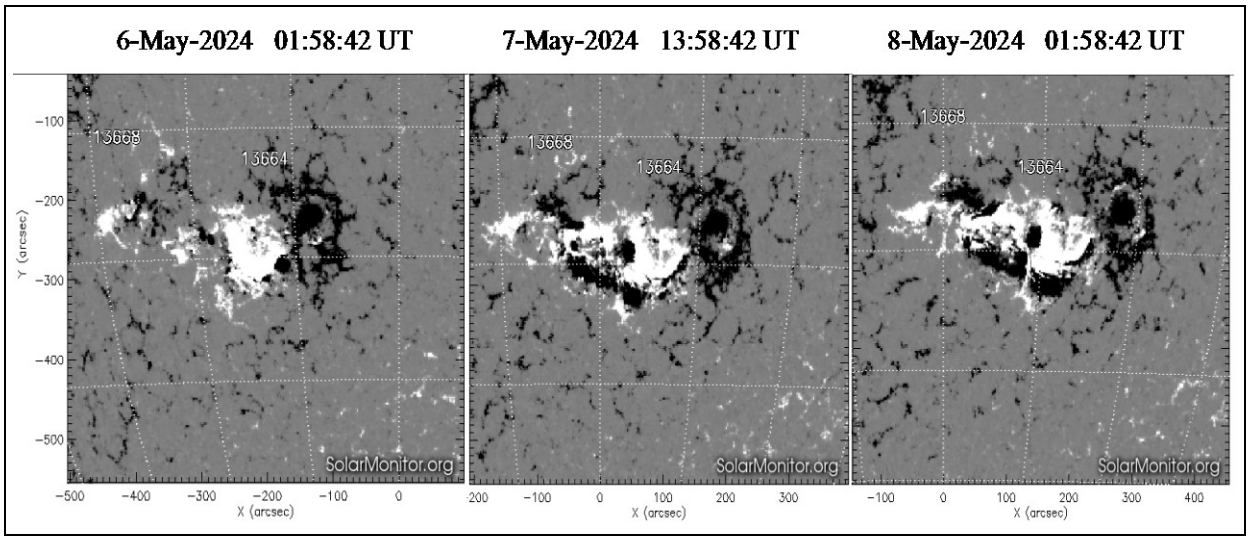

Figure 1a: AR13664 magnetograms obtained with the SDO/HMI instrument on May 6, 7 and 8, 2024. The positive and negative polarities are indicated by white and black colors, respectively.

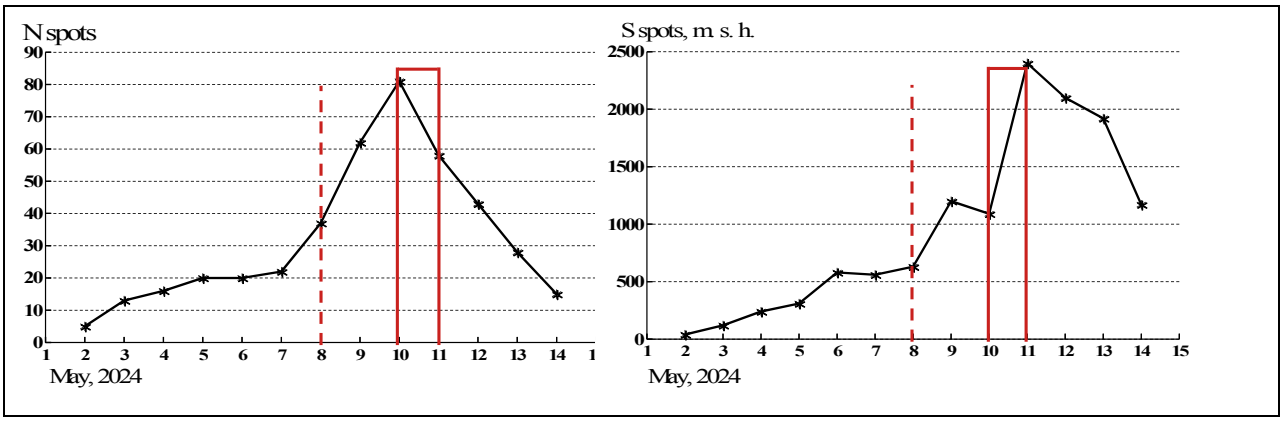

Figure 1b: Change in the number of sunspots (N) and the area occupied by them (S, m. s. h. is S, millionths of the solar hemisphere) during the first passage of AR13664 across the Sun's disk. The start time of the CME is marked by vertical dashed lines, the time of the storm by solid lines.

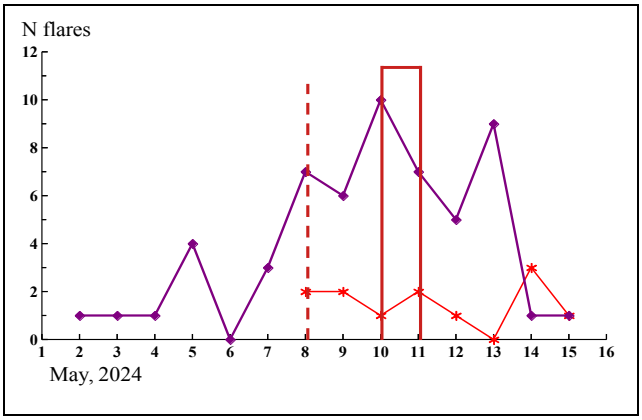

Figure 1c: Change in the number of M (purple curve) and X (red curve) class flares (N flares) over time in AR 13664. The start time of the CME is marked by vertical dashed lines, the time of the storm by solid lines

et al., 2024). The authors found that cannibal CMEs from AR 12887 interacting with CME from AR 12891 demonstrated increased geoeffectiveness compared to individual CMEs.

The geomagnetic storm ended on May, 12. It caused power outages and disrupted GPS and high-frequency radio communications. Auroras were seen in Europe, Asia, Mexico, and all 50 U. S. states, including Hawaii. Auroras were seen as far away as London and near San Francisco, California, as well as in many parts of Ukraine. AR 13664 passed across the solar disk two more times, but there were no more powerful ejections from it towards Earth. The development of the region in subsequent passages across the solar disk is described in (Kondrashova et al., 2024).

The most powerful geomagnetic storm since 2000 with a peak Dst index of -422 nT was on November 20, 2003. Its source was AR NOAA 10484 in its second pass across the Sun's disk. AR 10484 appeared on October 18, 2003

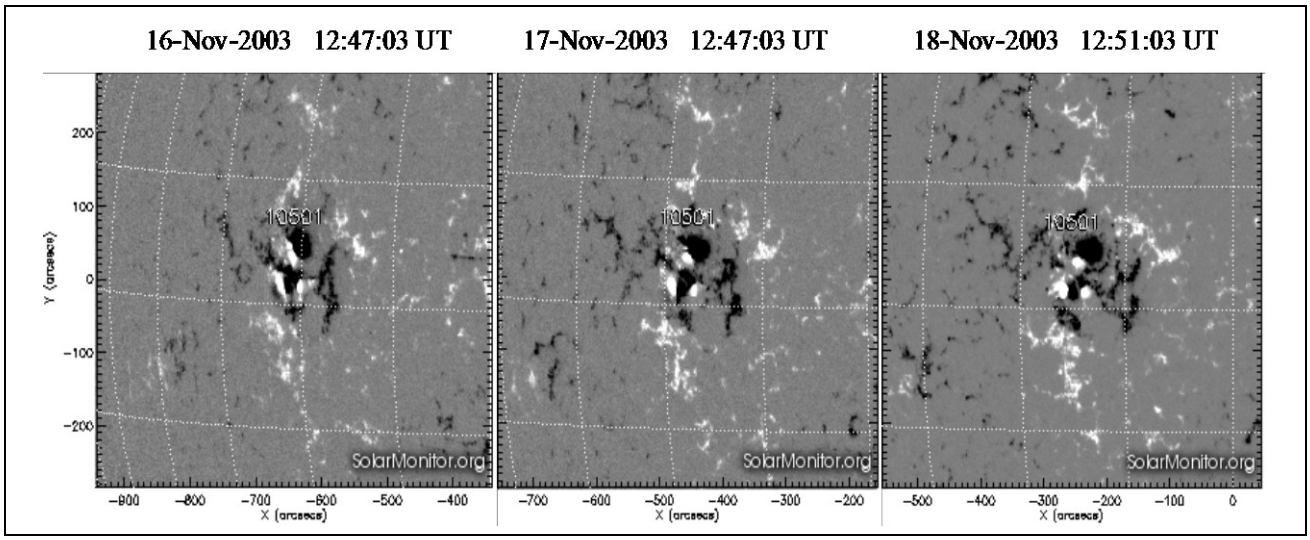

Figure 2a: MDI magnetograms for AR10501 on November 16, 17 and 18, 2003.

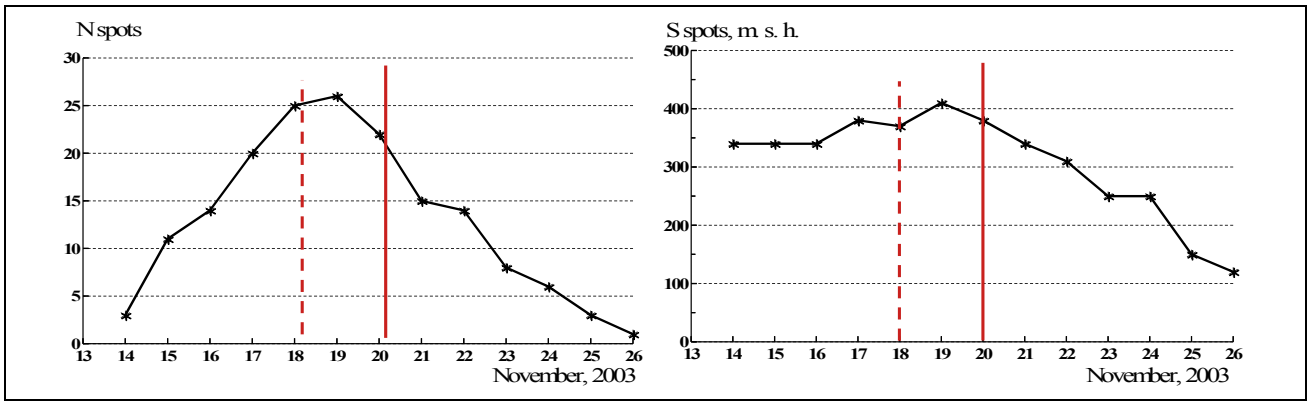

Figure 2b: the same as in Figure 1a, but in AR10501.

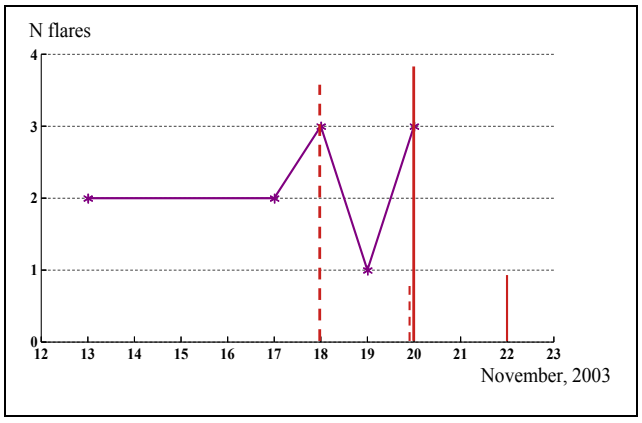

Figure 2c: Change in the number of M (purple curve) class flares (N flares) over time in AR10501.

during the declining phase of the 23rd solar cycle in the northern hemisphere of the solar disk and passed across the disk until October 31, 2003. Its maximum area was 1750 millionths of the hemisphere, and the maximum number of sunspots was 69. It had a complex magnetic configuration of the βγδ class. On October 19, 22, and 26, powerful X and M flares occurred in the AR, triggering CMEs. Despite this, no major geomagnetic storms occurred. On October 19 and 26, the region was located at the edges of the disk, and the ejections were directed past Earth. On October 22, the Bz component of the interplanetary magnetic field was directed north.

In the second pass through the disk, AR 10484 was renumbered as NOAA 10501. The AR 10501 passed across the solar disk from November 13 to November 26, 2003. On November 18, it experienced an M3.9 flare, which caused a powerful CME. Fig 2a shows the magnetograms obtained with the SOHO/MDI instrument on November 16-18, 2003, before the storm on November 20. The magnetic field configuration of the region was of βγ class, and became more complex on November 19 to the βγδ class. Fig. 2b, and Fig. 2c shows the changes in the number of sunspots, area, and the number of M class flares over time in AR 10501. The maximum number of sunspots was 26 and the area maximum was 410 millionths of the solar hemisphere on November 19. On November 18, the number of sunspots was 25 and the area was 370 millionths of the solar hemisphere. The flares of M1.8, M3.2 and M3.9 occurred in AR 10501 on this day.

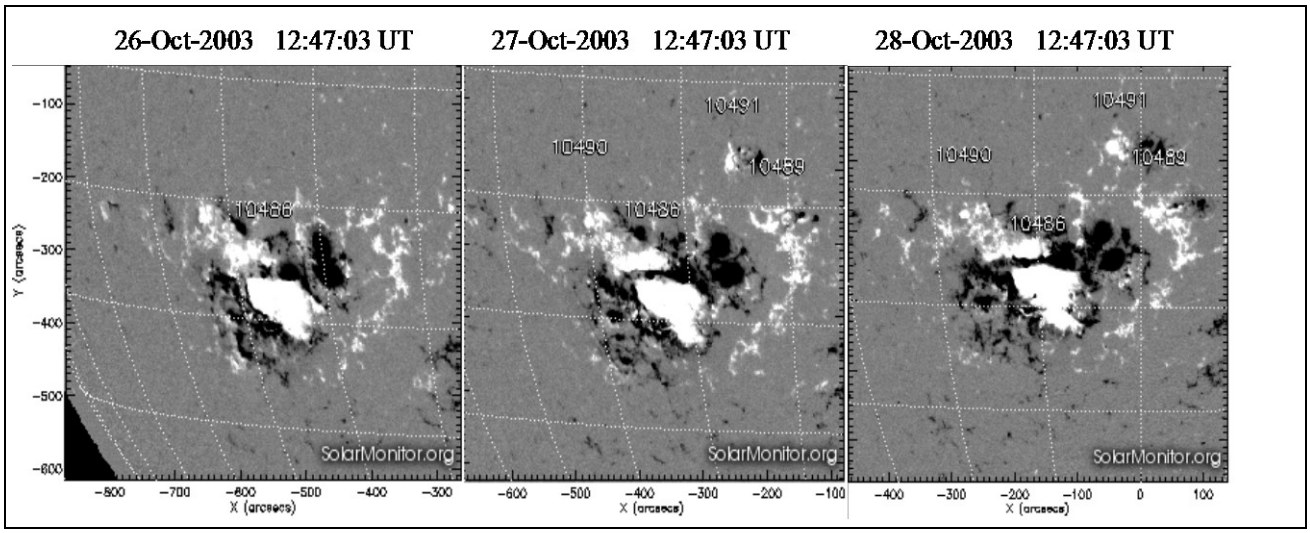

Figure 3a: MDI magnetograms for AR10486 on October 26, 27 and 28, 2003.

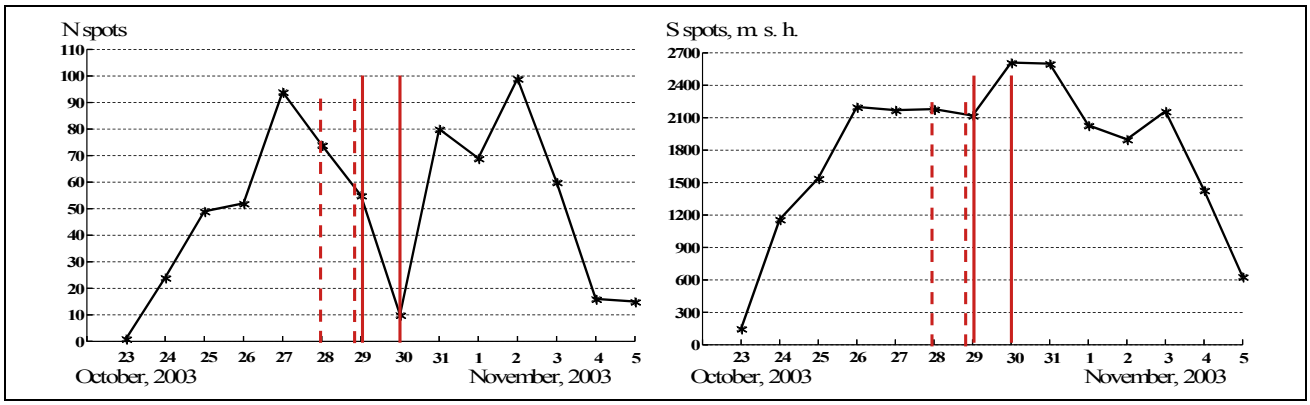

Figure 3b: the same as in Figure 1b, but in AR10486.

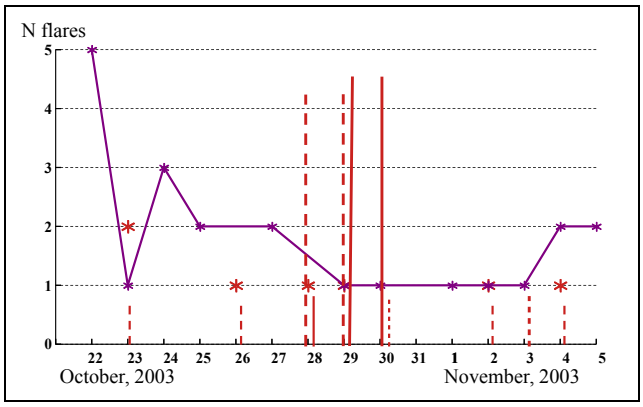

Figure 3c: Change in the number of M (purple curve) and X (red stars) class flares (N flares) over time in AR10486.

The extreme geomagnetic storm on November 20, 2003 became the fifth since 1957, the beginning of the space age. It was accompanied by a proton storm. During the peak of the storm, auroras were seen as far south as Florida, Michigan, and Wisconsin in the United States and Greece in Europe. In the days leading up to the storm, the solar wind stream affected the Earth's magnetic field, causing weak geomagnetic storms. The magnetosphere was already agitated, which may have intensified the extreme storm. Raghav et al. (2023) suggested that the CME that led to the November 20 event had an extremely flattened structure. It had less adiabatic expansion than usual in the compressed direction, which led to a strong magnetic field strength, high plasma density, high solar wind speed, high dynamic pressure, and a strong interplanetary electric field to the east. This may have contributed to the efficient transfer of plasma and energy to the Earth's magnetosphere.

3. Other extreme geomagnetic storms that occurred during the study period

NOAA 10486 was the most active region of Cycle 23 and was characterized by high flare activity. During its passage across the solar disk, it produced 7 X-class flares, about two dozen M-class flares, and 6 CMEs. The most powerful flares ever recorded occurred in it. It passed across the solar disk from October 23 to November 4, 2003 in the declining phase of the 23rd solar cycle. AR 10486 was part of a large active complex. The structure of the region was rapidly changing and becoming more complex. Its area and sunspot number increased rapidly

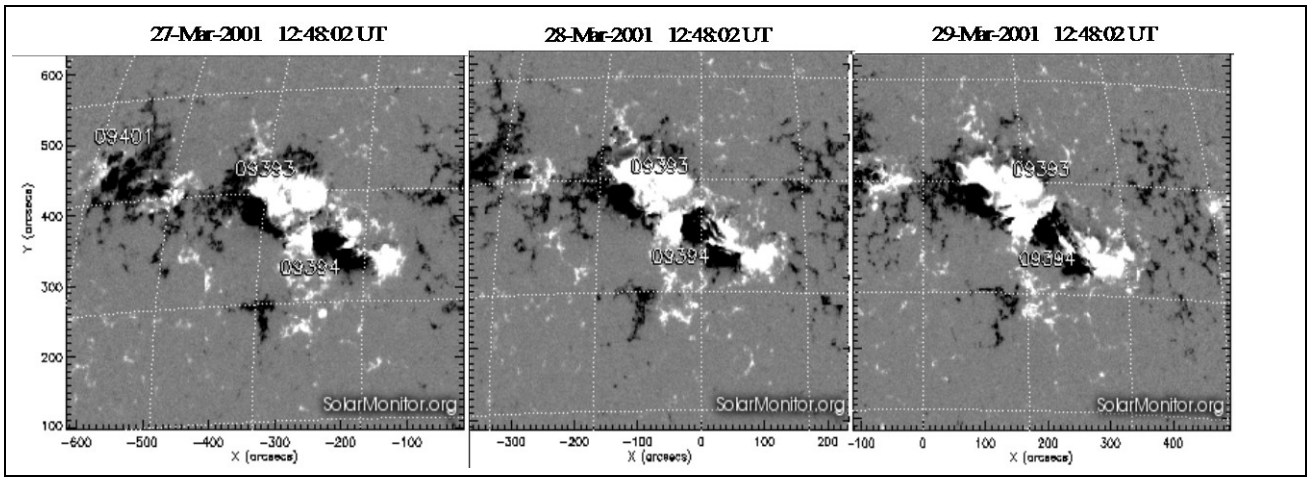

Figure 4a: MDI magnetograms for AR09393 on March 27, 28 and 29, 2001.

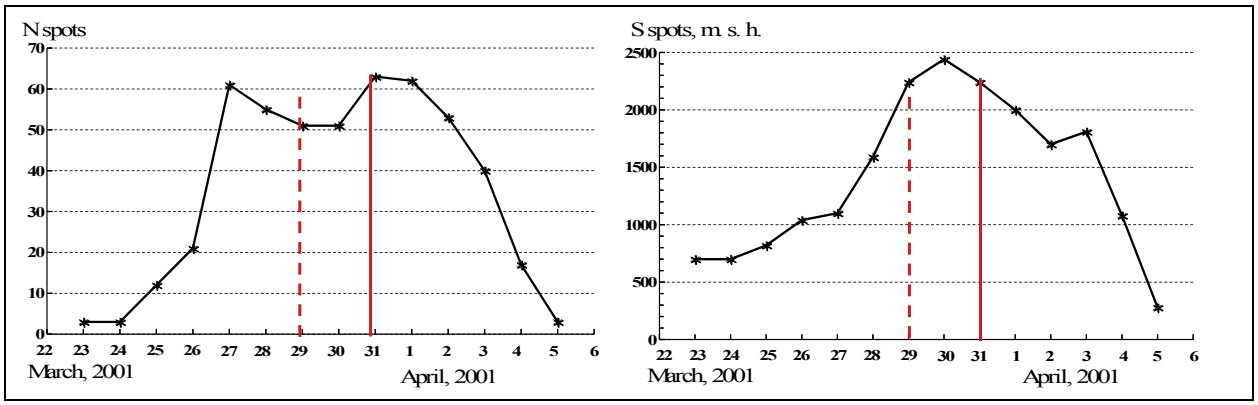

Figure 4b: the same as in Figure 1b, but in AR09393.

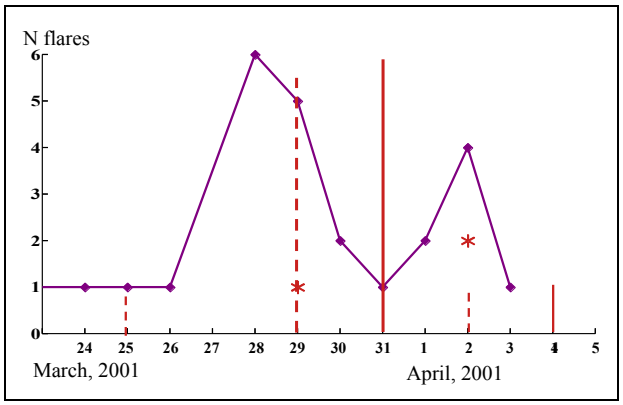

Figure 4c: the same as in Figure 3c, but for AR09393.

over time. The magnetic field structure changed over time and became increasingly complex. Magnetograms of the AR 10486 show the penetration of negative polarity to positive (Fig. 3a). The magnetic field configuration of the region was of class βγδ. The activity of the AR has increased with the appearance of δ-sunspots. On October 28, a flare X17 class occurred in the region, and on October 29, a flare X10 class. CMEs from these flares caused two geomagnetic storms with the minima Dst index of -353 nT and -383 nT on October 30. The changes in the number of sunspots, area, and the number of M and X class flares over time in AR 10486 are presented in Fig 3b and Fig 3c. The maximum number of sunspots was 99 and the area maximum was 2610 millionths of the solar hemisphere. On November 4, 2003 the X18+ flare caused a powerful CME, but there was no geomagnetic storm because the region was at the edge of the solar disk.

The AR 09393 was also very active. 24 M-class flares and 3 X-class flares occurred in it. It appeared on March 23, 2001 near the maximum of the 23rd solar cycle in the north hemisphere of the solar disk and passed along the disk to April 5, 2001. The region was part of a very large active complex. The magnetic field configuration of the region by March 25th had become more complex, from βγ to βγδ. Magnetograms of the AR obtained on March 27-29, 2001, before the CME, show penetration of negative polarity into positive polarity in several places (Fig. 4a). It is known that when δ-sunspots containing opposite polarities appear, powerful flares can occur. On March 28 the number of powerful flares has increased sharply. The powerful flares M4.3 on March 28 and X1.7 on March 29

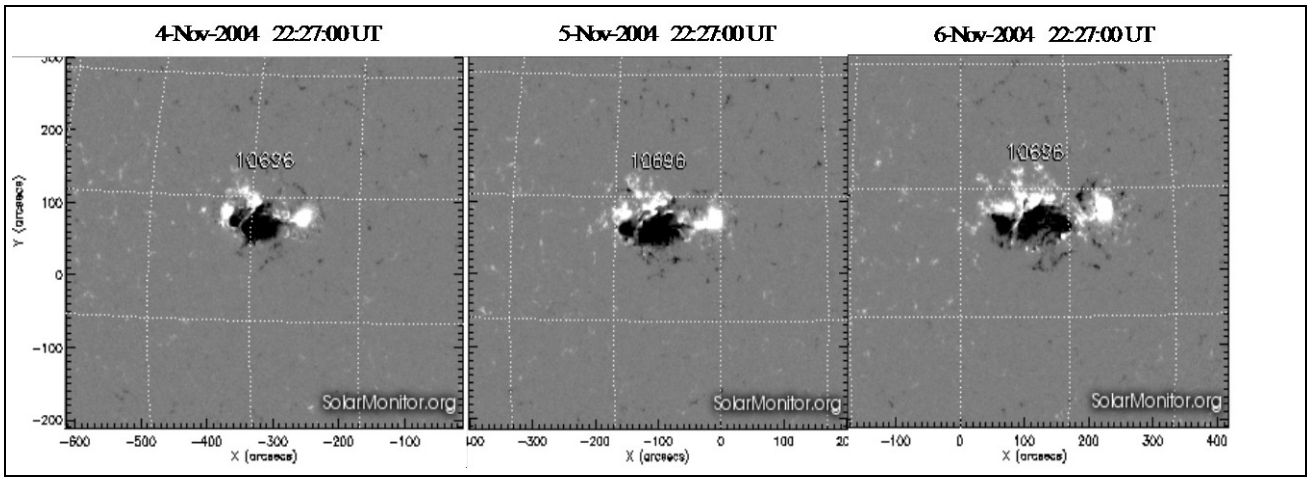

Figure 5a: MDI magnetograms for AR10696 on November 4, 5 and 6, 2004.

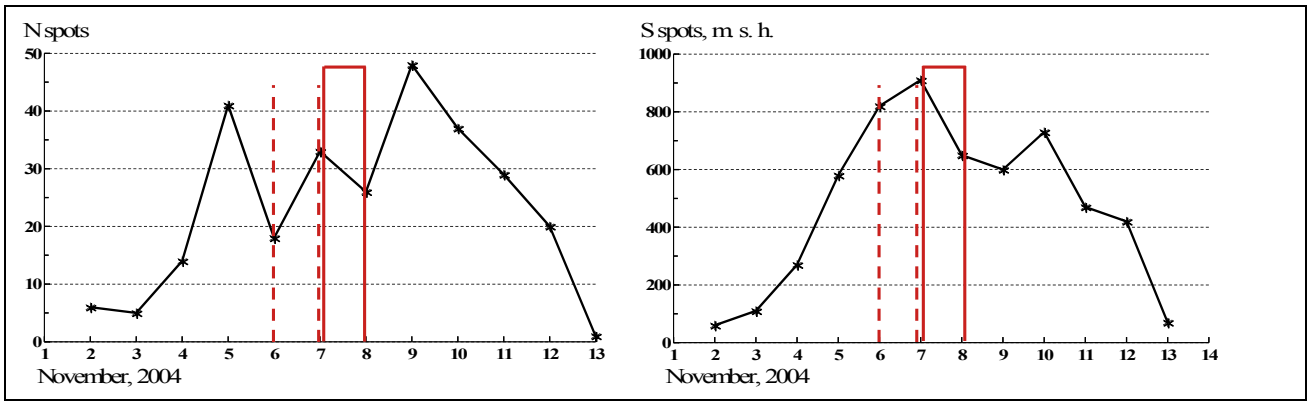

Figure 5b: the same as in Figure 1b, but in AR10696.

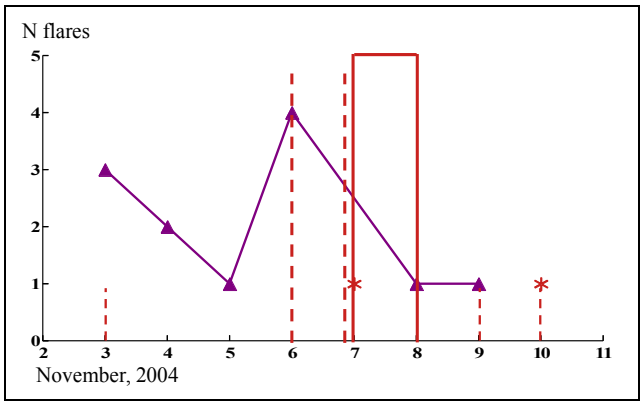

Figure 5c: the same as in Figure 3c but for AR10696.

in AR caused CMEs. The extreme storm with a minimum Dst of -387 nT began at 01:00 UT on March 31st when the first CME struck Earth's magnetosphere. A second CME struck magnetosphere at ~22.00 UT on March 31th and caused less strong storm with a peak Dst index of -284 nT. As the CME passed Earth, the interplanetary magnetic field suddenly turned north. X1.7 flare triggered a day-long S1-class proton storm. Changes in the number of sunspots, area and flares number in the AR 09393 region are shown in Fig. 4b and Fig. 4c. The maximum number of sunspots was 63 on March 31 and the area maximum was 2440 millionths of the solar hemisphere on March 30. On April 2, 2001, the most powerful X20-class solar flare since 1976 occurred, causing a powerful CME, but this region was at the edge of the disk, and a storm did not occur.

The AR 10696 produced 14 powerful flares of M and X class and six CMEs. It passed across the solar disk from November 1 to November 13, 2004, during the declining phase of the 23rd solar cycle, in the northem hemisphere. The region was growing rapidly. The structure of the magnetic field gradually became more complex. In the first days of the AR passage across the solar disk, the configuration of its magnetic field was of β class, and by November 5 it was already of βγδ class (Fig. 5a). The area and the number of sunspots were increasing (Fig 5b and Fig. 5c). The maximum number of sunspots was 48 and the area maximum was 910 millionths of the solar hemisphere. The number of powerful flares increased on November 6. On this day AR 10696 produced four powerful flares. M9.3-class flare erupted by CME, which caused extreme geomagnetic storm. The storm began at 22:00 UT on November 7, and Dst index reached a minimum of -374 nT on November 8. Auroras were observed as far south as Alabama and California in the United States.

4. Conclusion

Although extreme geomagnetic storms are rare, they cause enormous economic losses and pose a threat to human health. Their study and prediction is extremely important. In this work, we identified typical features of active regions where coronal mass ejections occurred, causing extreme geomagnetic storms, as follows:

– Active regions studied developed very quickly, their area and the number of sunspots increased rapidly.

– These ARs typically had a complex magnetic field configuration of βγδ class.

– They were often part of activity complexes.

– Their area, the number of sunspots and flares, on the day when a coronal mass ejection occurred were, close to the maximum.

– The flare activity of the ARs, caused by the emergence of new magnetic fluxes and their reconnection with the magnetic field of these regions, increased several days before the ejections. The ARs became the source of high-intensity flares of classes M and X. Whole series of powerful flares often occurred. Powerful flares created the largest CMEs and associated extreme geomagnetic storms.

– Cannibal CMEs increased the power and duration of the geomagnetic storms.

– The AR location near the central meridian contributes to greater geoeffectiveness of the CME.

– ARs with a small area and moderate flares can sometimes produce extreme storm.

Forecasting CMEs and storms is complicated by the many factors that contribute to their occurrence and determine their powerful. Improving the quality of forecasts requires improved ground-based and space-based observation techniques, as well as a comprehensive and detailed study of the magnetic field and morphological characteristics of the active regions, including those discussed in this paper. They can be useful in the extreme storms forecasting modeling, including using machine learning.

Acknowledgments. The authors are grateful to the referee for providing useful comments, which helped improve the quality of the manuscript. We thank the observing teams at the Kyoto geophysical observatory, SOHO, SDO, and GOES for providing free access to their results.

References

Carrington R. C.: 1859, *MNRAS*, **20**, 13.

Hayakawa H., Ebihara Y., Mishev A. et al.: 2025, *ApJ,* **979**, 49.

Hodgson R. M.: 1859, *MNRAS*, **20**, 15.

Jarolim R., Veronig A., Purkhart S. et al.: 2024, preprint (arXiv:2409.08124).

Jaswal P., Sinha S., Nandy D.: 2024, preprint (arXiv:2409.14752).

Kondrashova N. M., Pasechnik M. M., Osipov S. M. et al.: 2024, *OAP*, **37**, 112.

Liu Y. D., Hu H., Zhao X. et al.: 2024, *ApJ L,* **974**, L8.

MacTaggart D., Williams T., Aslam O.P.M.: 2024, preprint *(*arXiv:2410.15964)

Romano P., Elmhamdi A., Marassi A. et al.: 2024, *ApJ L*, **973**, L31.

Raghav A., Shaikh Z., Vemareddy P. et al.: 2023, *SoPh*, **298**, 64.

Soni S. L., Maharana A., Guerrero A. et al.: 2024, *A&A*, **686**, A23.

Wang R., Liu Y. D., Zhao X. et al.: 2024, *A&A*, **692**, A112.